Journal of Colloid and Interface Science 533 (2019) 598–603

Contents lists available at ScienceDirect

Journal of Colloid and Interface Science

journal homepage: www.elsevier.com/locate/jcis

Regular Article

Aggregation of Ag(0) nanoparticles to unexpected stable chain-like assemblies mediated by 2,2′-bipyridine decorated peptoids

Hagar Tigger-Zaborov, Galia Maayan *

Schulich Faculty of Chemistry, Technion – Israel Institute of Technology Technion City, Haifa 3200008, Israel

GRAPHICAL ABSTRACT

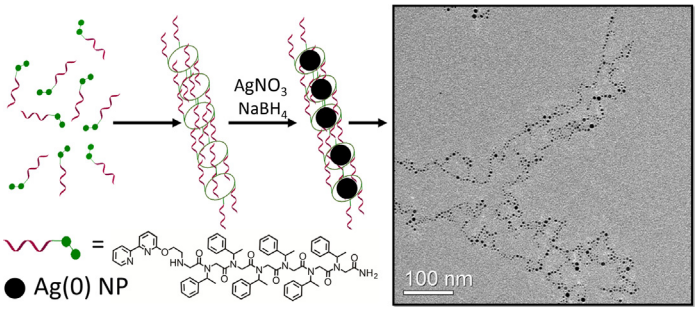

ARTICLE INFO

Article history:
Received 19 July 2018
Revised 26 August 2018
Accepted 27 August 2018
Available online 31 August 2018

Keywords:
Ag nanoparticles
Peptoid
Peptide
Aggregation
Self-assembly

ABSTRACT

We report a unique example of Ag(0) nanoparticles (NPs)-assemblies stabilized by 2,2-bipyridine (BP), via the incorporation of BP at the *N*-terminus of a peptoid heptamer bearing phenylethyl groups in the other positions. We show that this peptoid mediates the aggregation of the Ag(0) NPs into nanochain-like assemblies. Transmission electron microscopy, supported by UV–Vis spectroscopy analysis, revealed pre-assembly of the BP-peptoid oligomers into elongated pearl-like morphology, which serve as a template for the NPs. The fact that completely synthetic biomimetic oligomers can template and control the assembly of metal NPs, and specifically Ag(0), represents a conceptual mimic of the interaction between biomolecules and minerals for the production of nanostructured inorganic materials with complex morphologies.

1. Introduction

Controlling the aggregation of metal nanoparticles (NPs) is a key to the production of NP assemblies with different morphologies towards applications in optical sensing and biology [1–5]. In nature, specific peptides and proteins can mediate the nucleation, growth and morphology of bioinorganic materials and control their mineralization. This has inspired research on NPs aggregation mediated by biomimetic oligomers, also because the final assemblies benefit from the distinct physical and biocompatible properties of both components, resulting in unique functional materials [5]. Examples include peptide-like systems that are capable of mineralizing Ag(0) from Ag salts [6], colorimetric sensors for metal ions [5,7], DNA fragments [3,5] and volatile organic compounds [1], as well as materials for surface enhanced Raman scattering (SERS) [1,3,5]. For SERS applications, Au(0) and Ag(0) NPs are often used due to their ability to absorb light at the UV–Vis region [1], such that the NPs size and dispersion can be realized from the wavelength of the UV absorbance bands [1,5]. Specifically, dispersed Ag(0) NPs with diameter of 5 nm exhibit absorbance band near 400 nm, and upon their assembly, the absorbance band shifts

* Corresponding author.
E-mail address: gm92@tx.technion.ac.il (G. Maayan).

https://doi.org/10.1016/j.jcis.2018.08.094
0021-9797/

to the red spectrum [1]. Moreover, Ag(0) NPs can be manipulated to absorb between 300 and 1200 nm, by changing the shape and dispersion of the NPs [1]. In addition, Ag has a high thermal and electric conductivity relative to all the other metals, making it an ideal component for applications in materials science [1]. Ag is also cheaper than Au, thus it is an ideal candidate for commercial applications [1].

It was previously shown that 1,10-Phenanroline (Phen) is an excellent capping ligand for Ag(0) NPs [8–11]. Phen-capped Ag(0) NPs, however, exhibit strong tendency for uncontrolled aggregation [8–11]. The capability of other capping ligands based on pyridine rings, such as 2,2′:6′,2″-Terpyridine [12] and 2,2′-bipyridine (BP) [13] was also explored [14–18]. Previous SERS studies demonstrated that BP can be adsorbed on Ag(0) NPs surface [19,20]. The direct use of this chelator, however, as a capping ligand for metal NPs was not demonstrated, probably because it lacks the steric and electronic requirements for NPs stabilization. As a consequence, only a few examples of BP-capped metal NPs were reported and these include the use of mesoporous organosilica to provide the required steric hindrance for Au(0) NPs stabilization [15], the synthesis of Rh(0) NPs in presence of an ionic liquid as an electronic stabilizer [16] and the stabilization of Ag(0) NPs by a gel matrix that is composed of BP as well as of other ligands [18]. The stabilization of Ag(0) NPs exclusively by BP was not reported.

Assembly of metal NPs can be mediated by biopolymers and their mimics [5] including DNA [21–24], peptides [5,7,25,26], peptoids [10,11] and peptide nucleic acids (PNAs) [27,28,5] Among these, peptoids, *N*-substituted glycine oligomers, that are biocompatible and stable in various pH and temperature conditions, hold great promise in the development of nanomaterials [29]. Peptoids can be efficiently synthesized on solid support from numerous primary amines, including amine-bound metal-chelating ligands such as Phen [10,11,30,31], terpyridine [32], BP [33,34], hydroxyquinoline [35] and more [36]. It was anticipated that the backbone and pendent groups of peptoids incorporating capping ligands will be able to provide the steric hindrance required for metal(0) NPs stabilization. It was also shown that Ru(II) complexes from BP-decorated peptoids exhibit lower oxidation potential than this of $Ru(BP)_3$ suggesting that the peptoid scaffold is also able to electronically stabilize an embedded metal center [33]. Indeed, it was recently reported that Phen-decorated peptoids can stabilize Ag (0) NPs and mediate their assembly in acidic solutions [10]. Specifically, the addition of a reducing agent to a mixture solution of Ag (I) and a peptoid heptamer bearing one Phen at the *N*-terminus and six (S)-(-)-1-phenylethyl (*N*spe) groups as side chains, led to the formation of uniform Ag(0) NPs assemblies [10,11]. Moreover, the degree of NPs aggregation could be precisely controlled by modifying the sequences and/or length of the peptoid oligomers. In all these cases, however, only spherical or quasi-spherical assemblies were obtained [10,11].

Herein, we wished to gain control over the morphology of Ag(0) NP assemblies by exploring whether different capping ligands can lead to the formation of different aggregation pathways. To this aim, we choose to use a peptoid heptamer having one BP ligand at the *N*-terminus and six *N*spe side chains, similar to the Phen-decorated peptoid hexamer that was shown to mediate the aggregation of Ag(0) into spherical assemblies [10,11]. In contrast to various ligands used for the stabilization and assembly of Ag(0) NPs, the BP rings can switch from the transoid to the cystoid conformation, providing access to macrocyclic structures via weak intermolecular interactions between the aromatic rings. As BP alone cannot stabilize Ag(0), we anticipated that its incorporation within a peptoid bearing phenylethyl groups will enable both the NPs stabilization by steric, π-π interactions and electronic effects and the formation of assemblies with a unique morphology.

2. Experimental methodology

2.1. Materials

Rink Amide resin HL (100–200 mesh) was purchased from Novabiochem. Trifluoroacetic acid (TFA, 99.5+%) was purchased from Alfa Aesar. Bromoacetic acid (≥98%) was purchased from MERCK. Silver-Nitrate (99%), Sodiumborohydride (99%), Trisodium Citrate Dihydrate (≥99%), N,N′-diisopropylcarbodiimide (DIC, 99%), piperidine (99%), acetonitrile (ACN) and water HPLC grade solvents (≥99.9%), 6-Bromo-2,2′-bipyridine (97%), Ethanolamine (99%) and butanolamine (98%) were purchased from Sigma-Aldrich; N,N-Dimethylformamide (DMF, 99.8%) and Dichloromethane (DCM, 99.9%) solvents were purchased from Bio-Lab ltd. These reagents and solvents were used without additional purification, with the exception of DMF that was dried with molecular sieves.

2.2. Synthetic procedures

2.2.1. Synthetic procedures for capping ligands

2-(2,2′-bipyridine-6-yloxy)ethylamine was synthesized according to a similar procedure previously published [33]. To a solution of DMSO (5 ml) with KOH (0.28 gr) and ethanolamine (100 μL) 6-Bromo-2,2′-bipyridine (0.255 gr) was added and the solution was stirred for five hours at 50 °C (see SI). To The reaction mixture was then added 40 ml of DCM and washed three times with water, dried over Na_2SO_4 and the solvent was removed by evaporation (0.2 gr, yield 86%). The product was analyzed by ^{1}H NMR: (400 MHz, $CDCl_3$): δ 8.67 (1H,dd) δ 8.38 (1H,m) δ 8.00 (1H, d) δ 7.82 (1H,d) δ 7.70 (1H, t) δ 7.29 (1H,m) δ 6.80 (1H,d) δ 4.46 (2H,t) δ 3.13 (2H, t). ^{13}C NMR (100 MHz, $CDCl_3$) δ 163.35, 156.16, 153.37, 149.43, 139.22, 137.13, 123.90, 121.12, 113.69, 111.37, 67.98, 41.53. ESI-MS calculated: 215.3; found: 216.5.

Supplementary data associated with this article can be found, in the online version, at https://doi.org/10.1016/j.jcis.2018.08.094.

2-(2,2′-bipyridine-6-yloxy)butylamine was synthesized according to a similar procedure previously published [33]. To a solution of DMSO (5 ml) with KOH (0.17 gr) and 4-Amino-1-butanol (100 μL) 6-Bromo-2,2′-bipyridine (0.15 gr) was added and the solution was stirred for 36 h at 50 °C (see SI). To The reaction mixture was then added 40 ml of DCM and washed three times with water, dried over Na_2SO_4 and the solvent was removed by evaporation (0.11 gr, yield 65%). The product was analyzed by ^{1}H NMR: (400 MHz, $CDCl_3$): δ 8.57 (1H, d) δ 8.3 (1H,d) δ 7.94 (1H,d) δ 7.**71** (1H,t) δ 7.64 (1H, t) δ 7.20 (1H,t) δ 6.70 (1H,d) δ 4.48 (2H, t) δ 2.7 (2H,t) δ 2.29 (6H, s). ^{13}C NMR (100 MHz, $CDCl_3$) δ 163.10, 156.09, 153.30, 149.09, 139.42, 136.74, 123.48, 120.93, 113.75, 111.59, 67.39, 58.28, 45.95. ESI-MS calculated: 229.6; found: 230.1.

2.2.2. Preparation of peptoid oligomers

Peptoids were synthesized manually on Rink amide resin using the submonomer approach [37]. All peptoid oligomers were synthesized at room temperature. Typically, 100 mg of resin was swollen in DCM for 40 min before initiating oligomer synthesis. Multiple washing steps using DMF were performed between each step described below. De-protection of the resin was performed by addition of 20% piperidine solution (2 ml in DMF) and the reaction was allowed to shake at room temperature for 20 min. At the end of this reaction, piperidine was washed from the resin using DMF (3 ml × 3 over 1 min). Bromoacetylation was completed by adding 20 eq. bromoacetic acid (1.2 M in DMF, 850 μL) and 24 eq. of diisopropylcarbodiimide (200 μL); this reaction was allowed to shake at room temperature for 20 min. Following the reaction, the bromoacetylation reagents were washed from the resin using DMF (3 ml × 3 over 1 min), and 20 eq. of submonomer amine (1.0 M in DMF, 1 ml) were added. The amine displacement reaction

was allowed to shake at room temperature for 20 min and was followed by multiple washing steps (DMF, 3 ml g^{-1} resin) (3 × 1 min). The last amine displacement with 2-(2,2′-bipyridine-6-yloxy) ethylamine or with 2-(2,2′-bipyridine-6-yloxy) butylamine was performed for 1 h. or 60 h, respectively. To cleave the peptoid oligomers from solid support for preparative HPLC the beads were treated with 5 ml of 95% TFA in water for 30 min. The cleavage cocktail was evaporated under low pressure, re-suspended in 2 ml HPLC water:acetonitrile solvent and lyophilized overnight. The crude peptoids purified by HPLC (>95%).

2.2.3. Preparation of Ag(0) NPs

1 equiv. of aqueous $NaBH_4$ solution (10 mM) was added to 2 ml aqueous solution mixture containing 1 equiv. of **BP-P1** (10 mM in acetonitrile) and 6.4 equiv. of aqueous $AgNO_3$ (10 mM).

2.3. Characterization methods

All peptoids were analyzed by reversed-phase High Performance Liquid Chromatography (HPLC) equipped with an analytical C18(2) column, Phenomenex, Luna 5 μm, 100 Å, 2.0 × 50 mm) on a Jasco UV-2075 PLUS detector. A linear gradient of 5–95% ACN in water (0.1% TFA) over 10 min was used at a flow rate of 700 μL/min. Preparative HPLC was performed using a AXIA Packed C18(2) column (Phenomenex, Luna 15 μm, 100 Å, 21.20x100mm). Peaks were eluted with a linear gradient of 5–95% ACN in water (0.1% TFA) over 50 min at a flow rate of 5 ml/min. Mass spectrometry of peptoid oligomers was performed on a Advion expression CMS mass spectrometer, under electrospray ionization (ESI), direct probe ACN:H_2O (95:5), flow rate 0.2 ml/min. UV measurements were performed using an Agilent Cary 60 UV–Vis spectrophotometer, a double beam, Czerny-Turner monochromator. Transmission Electron Microscope (TEM) micrographs were taken by TEM Tecnai G^2 T20 200KeV, with a LaB_6 electron source and an FEI Supertw in Objective Lens, a plate camera, and a 1Kx1K multi-scan charge-coupled device (CCD). TEM specimens were prepared at Cu-200 mesh grid, coated by formaver and a carbon layer. Negative stained specimens were dyed by Phosphotungstic acid (2%). Cryo-TEM micrographs were taken by FEI Talos 200C, Field Emission Gun (FEG)-equipped cryo-dedicated high-resolution TEM. Cryo-TEM samples were prepared in the controlled environment vitrification system (CEVS) at 25 °C, and at 100% relative humidity to prevent evaporation from the specimen. In the specimen preparation chamber, a carbon-coated holey carbon polymer film, supported on a 200 mesh TEM grid was held by tweezers. A drop of the sample was placed on the film, and blotted to form a thin film of liquid. The specimen was then vitrified by quickly plunging into liquid ethane at its freezing point. After vitrification the sample was kept in liquid nitrogen until transfer into the Cryo-TEM for imaging. Raman spectra were obtained by using a confocal micro-Raman LabRam High Resolution (HR) instrument from Horiba Scientific in backscattering geometry with a 50× objective mounted on an Olympus optical microscope. The excitation line was provided by a VIS 532 nm laser (Torus, 100 mW) and a Peltier cooled CCD (1024 × 256 pixels) was used as detector. The calibration is initially made using a silicon reference at 520 cm^{-1}, which gives a peak position resolution of less than 1 cm^{-1}. For each acquisition average of five spectra and acquisition time of 10 s was performed. The spectra were linearly baseline corrected for clarity. Data processing was done with the softwares TIA, Gtan Digital Micrograph, Excel and KaleidaGraph.

3. Results and discussion

Solid-phase peptoid synthesis via the "submonomer" method (Fig. 1a) enables the facile incorporation of numerous primary amines [38,39] within the peptoid scaffold including un-protected bipyridine-based ligands [30–32,34,36]. Initially, we have synthesized the heptamer **BP-P1** (Fig. 1b), from the BP amine derivative 2-(2,2′-bipyridine-6-yloxy) ethylamine prepared according to a previously reported procedure [33]. The peptoid **BP-P1** was generated on solid support by the submonomer method, analyzed by HPLC, cleaved from the resin, purified by HPLC (>95%) and its identity was verified by ESI mass spectrometry (MS, see SI). **BP-P1** was further used for the direct synthesis of Ag(0) NPs [11]. In short, 1 equiv. of aqueous $NaBH_4$ solution (10 mM) was added to 2 ml aqueous solution mixture containing 1 equiv. of **BP-P1** (10 mM in acetonitrile) and 6.4 equiv. of aqueous $AgNO_3$ (10 mM). This amount of $AgNO_3$ (6.4 equiv.) was the minimum required to engage all the peptoid molecules in solution for the NPs stabilization, and the maximum required for Ag(0) NPs formation. A lower ratio of peptoid:$AgNO_3$ resulted in immediate NPs precipitation. Upon addition of $NaBH_4$, an immediate yellow-orange color appeared. The NPs solution was kept unstirred for 24 h and the remained yellow-orange. The UV–Vis spectrum of this solution exhibited an absorbance band near 416 ± 2 nm (see SI), reflecting a red shift from the absorption band of well-dispersed Ag(0) NPs (near 400 nm), implying that Ag(0) NP assemblies were obtained [1]. The fact that only one such band was observed suggests that only one population of assemblies is present in solution. As a control, we have conducted the same reaction with 1 equiv. of BP instead of **BP-P1**, and in this case the initially formed yellow color disappeared immediately, and the UV–Vis spectrum of this solution showed a band near 284 nm corresponding the free BP ligand. These results indicate that any formed NPs precipitated immediately because they could not be stabilized by BP alone.

Transmission electron microscope (TEM) analysis of the **BP-P1** stabilized Ag(0) NPs revealed the formation of long branched NP-nanochains with length of about 1–2 μm, which contain NPs with an average diameter of 3.8 ± 1.3 nm (Fig. 2a). This is a remarkable result because the morphology of these aggregates is distinctly different from the spherical morphology of previously reported Ag(0) NP assemblies mediated by peptoids [10,11]. In order to eliminate the possibility that the NPs aggregation occurs as a result of fast solvent evaporation on the grid during sample preparation for TEM analysis, Cryo-TEM measurements were performed in a frozen solution. The obtained micrograph was almost identical to

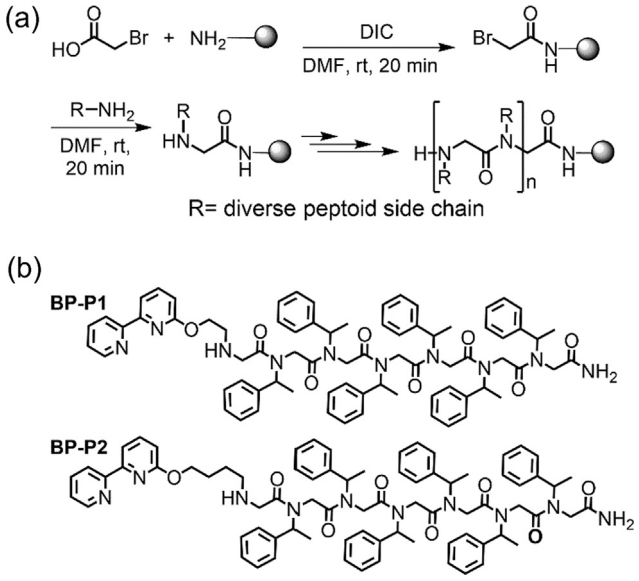

Fig. 1. (a) Solid-phase synthesis of peptoid oligomers by the submonomer method. (b) Chemical structures of peptoid oligomers **BP-P1** and **BP-P2**.

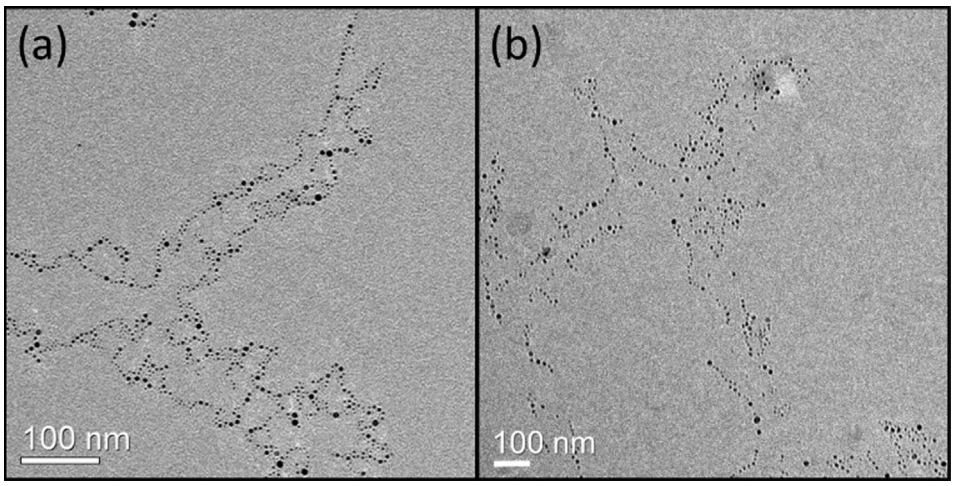

Fig. 2. (a) TEM micrograph and (b) Cryo-TEM micrograph of Ag(0) NP-assemblies mediated by **BP-P1**.

the one taken from a dried sample confirming the presence of the nanochains in solution (Fig. 2b).

We have previously showed that a peptoid heptamer bearing only phenylethyl side-chains that is lacking a capping ligand, cannot lead to the assembly of Ag(0) NPs [11]. As BP alone cannot stabilized Ag(0) NPs (see above details regarding our control UV–Vis experiment), we wanted to verify that the Ag(0) are bound to BP within the peptoid. To this aim, we decided to perform a Raman spectroscopy analysis of the **BP-P1**-capped Ag(0) NPs solution, and compare it to the spectrum documented in the literature, which identified the vibration between Ag(0) surface and pyridine nitrogen as a stretching band at 240 cm^{-1} [8,40]. In our experiment, a sample from the **BP-P1**-capped Ag(0) NPs solution was placed on a silicon surface and this sample was analyzed by Raman spectroscopy. The resulting spectra (Fig. 3) clearly exhibits a band at 241 cm^{-1}, indicating the existence of an Ag(0)-(pyridine)N interaction.

It was previously reported on the stabilization of Ag(0) NPs by a gel matrix containing BP as well as other pyridine-based ligands. In this case, the Ag(0) NPs were formed via the reduction of Ag(I) ions coordinated by these ligands within the gel matrix. In order to explore the possibility that the Ag(0) NPs nanochains are formed

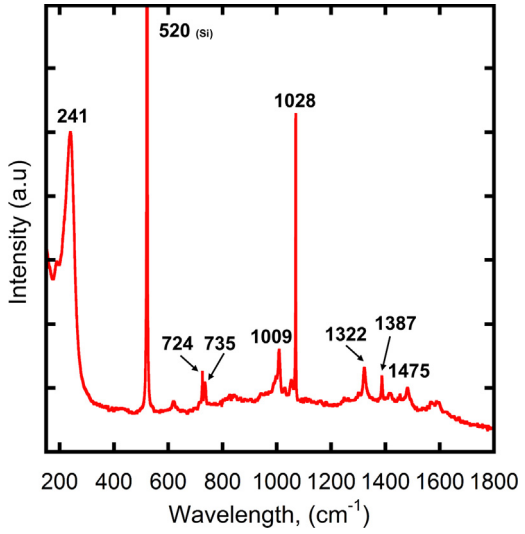

Fig. 3. Raman spectrum of Ag(0) NPs assemblies mediated by **BP-P1**, performed in water on a silicon surface. The band near 520 cm^{-1} refers to the silicon vibration.

in a similar process, we analyzed the UV–Vis spectra of a solution containing only **BP-P1** before and after the addition of $AgNO_3$ in the same equiv. ratio and concentrations that were used for the preparation of the Ag(0) NPs solution, but without the addition of the reducing agent $NaBH_4$. Interestingly, the two spectra were identical, exhibiting one band at 284 nm (corresponding to the free peptoid), suggesting that Ag(I) does not bind the peptoid (Fig. S7). Thus, we could conclude that the coordination complex Ag(**BP-P1**) was not formed and that the Ag(0) NPs in our solution mixture are obtained upon the reduction of $AgNO_3$ in the presence of **BP-P1**. Accordingly, chain-like assemblies could be formed in one of two possible processes: (i) pre-organization of the peptoids into nanochains templates followed by Ag(0) NPs aggregation into these templates (Fig. 4a, 1), or (ii) formation of Ag(0) NPs stabilized by the peptoid molecules, which further aggregate via intermolecular interactions between the peptoid oligomers (Fig. 4a, 2). In both cases, because BP is not planar and exists as a transoid in solution [41], the intermolecular interactions between the pyridine groups from different oligomers can lead to the formation of macrocycles (see Fig. 4a, bottom left). This possibility is also supported by literature reports demonstrating that BP derivatives-based foldamers could form macrocyclic structures [42]. In our case, the macrocycles are bounded to the peptoid via the flexible linker. Thus, these linkers can be arranged above and below the plain of the macrocycle and form assemblies with other such macrocycles via intermolecular aromatic interactions between different peptoid backbones leading to the formation of chain-type morphology (Fig. 4a). A UV–Vis spectrum, measured immediately after addition of $NaBH_4$, showed only a band near 416 nm indicative for assembled NPs. This result excludes the possibility that well-dispersed Ag(0) NPs are generated first and suggests that the Ag(0) NPs aggregate as they are formed. Moreover, analyzing a sample from a solution containing only **BP-P1** by TEM, using negative staining, showed elongated chain-like peptoid assemblies with an average length of about 350–600 nm (Fig. 4b). We therefore suggest that the formation of the Ag(0) NPs cannot be separated from the formation of the Ag(0) NPs assemblies, and propose the following mechanism for their formation: the peptoid molecules first form chain-like templates in solution and only after the reducing agent sodium $NaBH_4$ is added to these organic templates in solution, the Ag ions are reduced to Ag(0) and these start to aggregate to form NPs inside the templates by binding to the BP nitrogen atoms, as we showed by Raman spectroscopy (Fig. 4a, 1). A similar process was previously suggested as an explanation for the aggregation of metal NPs mediated by peptides [25,26].

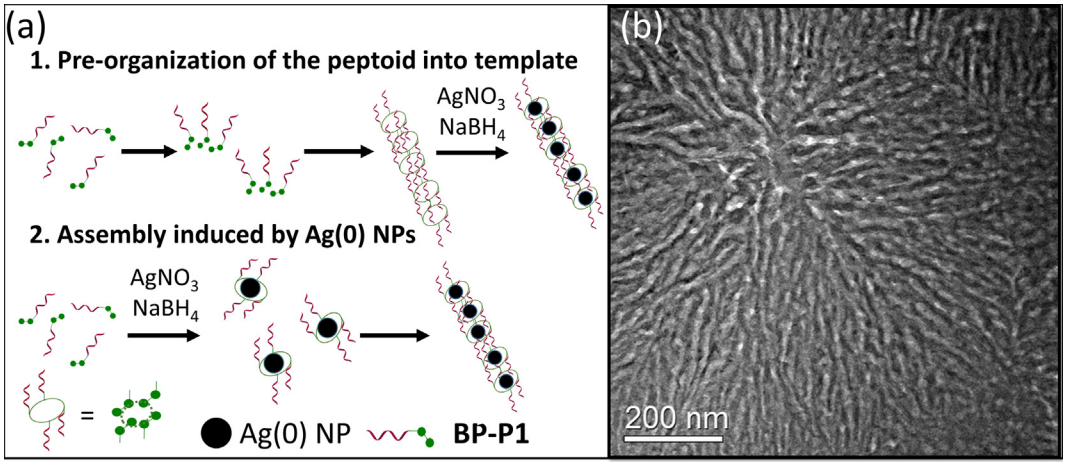

Fig. 4. (a) Two possible mechanisms for the assembly of Ag(0) NPs mediated by **BP-P1**. (b) TEM micrograph of **BP-P1** using the negative staining technique, showing elongated chain-like peptoid assemblies.

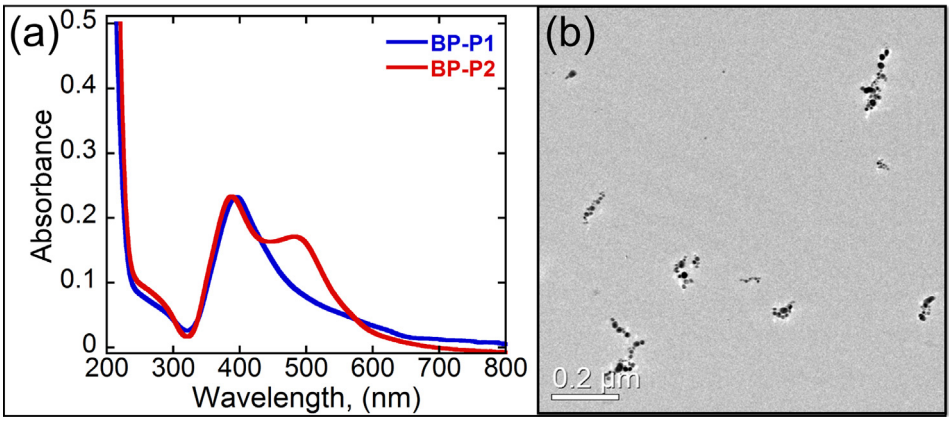

Fig. 5. (a) UV–Vis spectrum of Ag(0) NP-assemblies mediated by **BP-P1** (blue) or **BP-P2** (red) taken 24 h after all the reactants were combined in solution. (b) TEM micrograph of Ag(0) NP-assemblies mediated by **BP-P2**.

Finally, we wished to explore whether we could control the length of the nanochains by changing the length of the linker between the BP capping ligand and the peptoid. Specifically, we anticipated that a longer linker would enable the formation of longer nanochains. To test this assumption, we have prepared the peptoid heptamer **BP-P2** (Fig. 1b), from the BP amine derivative 2-(2,2′-bipyridine-6-yloxy) butylamine, which its linker is two carbon-carbon bonds longer than this of **BP-P1**. This peptoid was also synthesized on solid support via the "submonomer" method, analyzed by HPLC, cleaved from the resin, purified by HPLC (>95%) and its identity was verified by ESI MS (see SI). Direct synthesis of Ag(0) NPs in the same conditions as with **BP-P1** resulted in a UV–Vis spectrum, which showed two absorption bands near 411 and 482 nm (Fig. 5a). This spectrum suggests the formation of non-uniform assemblies, with at least two populations different in their size. Indeed, TEM measurements revealed Ag(0) NP assemblies with mixed morphology, demonstrating the formation of short nanochains with an average length of 200 nm, as well as a few elliptical shaped NP-assemblies, with an average diameter of 73 nm, (Fig. 5b). Within these assemblies, the Ag(0) NPs diameter ranged between 1 and 30 nm, divided into two populations (see Fig. S18): NPs with a diameter <10 nm (3.7 ± 2.4 nm in average) and NPs with a diameter >10 nm (20.6 ± 4.35 nm in average). These NPs, however, were unstable, and precipitated after a few hours. This instability could be stems from the presence of a longer linker between BP and the peptoid scaffold, which might reduce the ability of the peptoid to contribute the electron density required for electronic NPs stability. Another possibility is that this longer linker is too flexible to allow for the self-assembly described in Fig. 4. Attempts to incorporate BP ligand via a shorter linker were unsuccessful, probably because side reactions that take place on the pyridine rings during peptoid synthesis.

4. Conclusions

To conclude, we succeeded to demonstrate that synthetic biomimetic oligomers, peptoids, can template and control the assembly of metal NPs, specifically Ag(0) NPs, which typically exhibit low stability. Based on TEM and UV–Vis, we show that by using the peptoid **BP-P1** we can mimic the biological concept of mineralizing metal ions: we demonstrate the initial formation of an organic template that do not bind Ag(I) ions, and only upon the addition of a reducing agent, Ag(0) NPs are formed directly in the template, and are stabilized in a pearl-like morphology by the BP ligand. This morphology is unique because other Phen-peptoids could only mediate the assembly of NPs into sphere-like morphology, and this could not be controlled by modifying the peptoids sequence or length [11]. Moreover, other reports on the formation of

chain-like NPs assemblies did not show that the formation of these assemblies occurs via a template [17]. To this end, our work represents an exciting example of biomimetic chemistry because it conceptually emulating the interaction between biomolecules and minerals for the production of nanostructured inorganic materials with complex morphologies. We therefore believe that this work can make an impact in the fields of biomimetic chemistry, nanomaterials and self-assembly, towards applications in sensing. Future work related to this study will therefor focus on SERS of small molecules and toxins.

Acknowledgements

The authors thank the Russell Berrie Nanotechnology Institute (RBNI) for financially supporting the TEM and the Cryo-TEM measurements. The authors thank Dr. Yaron Kauffmann and Mr. Michael Kalina for their assistance with TEM measurements. The authors thank Dr. Naama Koifman for her assistance with Cryo-TEM measurements. The authors thank Dr. Rachel Edrei for her assistance with the Raman measurements.

References

[1] M. Rycenga, C.M. Cobley, J. Zeng, W. Li, C.H. Moran, Q. Zhang, D. Qin, Y. Xia, Chem. Rev. 111 (2011) 3669–3712.
[2] D.D. Evanoff, G. Chumanov, ChemPhysChem 6 (7) (2005) 11221–11231.
[3] N.L. Rosi, Chad A. Mirkin, Chem. Rev. 105 (4) (2005) 1547–1562.
[4] K.M.L. Taylor-Pashow, J.D. Rocca, R.C. Huxford, W. Lin, Chem. Commun. 46 (2010) 5832–5849.
[5] H. Tigger-Zaborov, G. Maayan, Org. Biomol. Chem. 13 (2015) 8978–8992.
[6] C.J. Carter, C.J. Ackerson, D.L. Feldheim, ACS Nano 7 (2010) 3883–3888.
[7] (a) S. Si, M. Raula, T.K. Paira, T.K. Mandal, ChemPhysChem 9 (11) (2008) 1578–1584;
(b) S. Si, A. Kotal, T.K. Mandal, J. Phys. Chem. C 111 (2007) 1248–1255.
[8] M. Muniz-Miranda, J. Phys. Chem. A 104 (2000) 7803–7810.
[9] (a) C.R. Mayer, E. Dumas, F. Sécheresse, Chem. Commun. (2005) 345;
(b) C.R. Mayer, E. Dumas, F. Miomandre, R. Méallet-Renault, F. Warmont, J. Vigneron, R. Pansu, A. Etcheberry, F. Sécheresse, New J. Chem. 30 (2006) 1628–1637.
[10] G. Maayan, L. Liu, Pept. Sci 96 (2011) 679–687.
[11] H. Tigger-Zaborov, G. Maayan, J. Colloid Interface Sci. 508 (2017) 56–64.
[12] U.S. Schubert, C. Eschbaumer, Angew. Chem. 41 (16) (2002) 2892–2926.
[13] C. Kaes, A. Katz, M.W. Hosseini, Chem. Rev. 100 (2000) 3553–3590.
[14] M. Pruskov, V. Sutrová, M. Šlouf, B. Vlčková, J. Vohlídal, I. Šloufová, Langmuir 33 (2017) 4146–13590.
[15] N. Ishito, K. Nakajima, Y. Maegawa, S. Inagakic, A. Fukuoka, Catalysis Today 298 (2017) 258–4156.
[16] B. Lger, A. Denicourt-Nowicki, A. Roucoux, H. Olivier-Bourbigoub, Adv. Synth. Catal. 350 (2008) 2631–2638.
[17] O.M. Piepenbrock, N. Clarke, J.W. Steed, Soft Matter 7 (2011) 2412–2418.
[18] R. Tatikonda, K. Bertula, Nonappa, S. Hietala, K. Rissanen, Matti Haukka, Dalton Trans. 46 (2017) 2793–2802.
[19] M. Khanafer, I. Izquierdo-Lorenzo, S. Akil, G. Louarn, J. Toufaily, T. Hamieh, P. Adam, S. Jrad, ChemistrySelect 1 (2016) 1201–1209.
[20] G. Sbrana, N. Neto, M. Muniz-Miranda, M. Nocentini, J. Phys. Chem. 94 (1990) 3706–3710.
[21] C.A. Mirkin, R.L. Letsinger, R.C. Mucic, J.J. Storhoff, Nature 382 (1996) 607–609.
[22] X.G. Peng, K.P. Johnsson, A.P. Alivisatos, Nature 382 (1996) 609–611.
[23] E. Auyeung, J.I. Cutler, R.J. Macfarlane, M.R. Jones, J. Wu, G. Liu, K. Zhang, K.D. Osberg, C.A. Mirkin, Nat. Nanotech. 7 (2012) 24–28.
[24] J.S. Lee, A.K. Lytton-Jean, S.J. Hurst, C.A. Mirkin, Nano Lett. 7 (2007) 2112–2115.
[25] (a) A.D. Merg, J. Slocik, M.G. Blaber, G.C. Schatz, R. Naik, N.L. Rosi, Langmiur 31 (2015) 9492–9501;
(b) L. Hwang, C.L. Chen, N.L. Rosi, Chem. Commun. 47 (2011) 185–187;
(c) C.L. Chen, N.L. Rosi, J. Am. Chem. Soc. 132 (2010) 6902–6903;
(d) C.L. Chen, N.L. Rosi, Angew Chem. 49 (2010) 1924–1942;
(e) C. Zhang, C. Song, H.C. Fry, N.L. Rosi, Nanoscale 6 (2014) 12328–12332;
(f) C. Zhang, C. Song, H.C. Fry, N.L. Rosi, Chem. Eur. J. 20 (4) (2014) 941–946;
(g) C. Song, M.G. Blaber, G. Zhao, P. Zhang, H.C. Fry, G.C. Schatz, N.L. Rosi, Nano Lett. 13 (7) (2013) 3256–3261.
[26] E.D. Sone, S.I. Stupp, J. Am. Chem. Soc. 126 (40) (2004) 12756–12757.
[27] F. Wang, H.B. Shen, J. Feng, H.F. Yang, Microchim. Acta 153 (2006) 15–20.
[28] X. Su, R. Kanjanawarut, Acs Nano 3 (2009) 2751–2759.
[29] R. Li, A. Smoyakova, G. Maayan, J. Rimer, Chem. Mat. 29 (2017) 9536–9546.
[30] P.J. Kaniraj, G. Maayan, Chem. Commun 51 (2015) 11096–11099.
[31] D. Chandra Mohan, A. Sadhukha, G. Maayan, J. Catal. 355 (2017) 139–1114.
[32] (a) M. Baskin, G. Maayan, Chem. Sci. 7 (2016) 2809–2820;
(b) G. Maayan, B. Yoo, K. Kirshenbaum, Tetrahedron Lett. 49 (2) (2008) 335–338.
[33] M. Baskin, L. Panz, G. Maayan, Chem. Commun. 52 (2016) 10350–10353.
[34] T. Ghosh, N. Fridman, M. Kosa, G. Maayan, Angew. Chem. Int. Ed. 57 (2018) 7703–7707.
[35] (a) M. Baskin, G. Maayan, Biopolymers, Pept. Sci. 104 (2015) 577–2820;
(b) G. Maayan, M.D. Ward, K. Kirshenbaum, Chem. Commun. (2009) 56–58;
(c) L. Zborovsky, A. Smolyakova, M. Baskin, G. Maayan, Chem. Eur. J. 24 (2018) 1159–1167.
[36] T. Zabrodski, M. Baskin, P.J. Kaniraj, G. Maayan, Synlett (2015) A1–A17.
[37] R.N. Zuckermann, J.M. Kerr, S.B.H. Kent, W.H. Moos, J. Am. Chem. Soc. 114 (1992) 10646–10647.
[38] P.J. Kaniraj, G. Maayan, Org. Lett. 17 (2015) 2110–2113.
[39] C.M. Darapaneni, P.J. Kaniraj, G. Maayan, Org. Biomol. Chem. 16 (2018) 1480–1488.
[40] A. De Bonis, G. Compagnini, R.S. Cataliotti, G. Marletta, J. Raman Spectrosc. 30 (1999) 1067–1071.
[41] D.J. Hill, M.J. Mio, R.B. Prince, T.S. Hughes, and, J. S. Moore Chem. Rev. 101 (12) (2001) 3893–4012.
[42] (a) F. Heirtzler, M. Neuburger, K. Kulike, J. Chem. Soc., Perkin Trans. (2002) 809–820;
(b) F.R. Heirtzler, M. Neuburger, M. Zehnder, S.J. Bird, K.G. Orrell, V. Sik, Dalton Trans. (1999) 565–574.